Available online at www.sciencedirect.com
ScienceDirect
International Journal of Heat and Mass Transfer 51 (2008) 1551–1561
International Journal of HEAT and MASS TRANSFER
www.elsevier.com/locate/ijhmt

Investigation of a large top wall temperature on the natural convection plume along a heated vertical wall in a square cavity

W. Wu, D. Ewing, C.Y. Ching *

Department of Mechanical Engineering, McMaster University, Hamilton, Ontario, Canada L8S 4L7

Received 25 August 2006; received in revised form 1 December 2006
Available online 10 September 2007

Abstract

The characteristics of the laminar natural convection in an air-filled square cavity heated and cooled on the side walls was studied for cases where the temperature of the top wall was significantly larger than the heated vertical wall. Experiments were performed for a horizontal Grashof number of 1.3×10^8, and non-dimensional top wall temperatures from 1.4 to 2.3. The results show that the plume formed on the heated vertical wall separated from this wall before reaching the top wall. As a result, three different regions were observed in the cavity: a stratified core region, a buoyant plume region, and a highly stratified region above the plume after it had separated from the vertical wall. The highly stratified region above the plume became larger and more stable with an increase of the top wall temperature, stabilizing the motion of the plume across the cavity. The similarity solutions developed by Kulkarni et al. [A.K. Kulkarni, H.R. Jacobs, J.J. Hwang, Similarity solution for natural convection flow over an isothermal vertical wall immersed in thermally stratified medium, Int. J. Heat Mass Transfer 30 (1987) 691–698] to characterize the natural convection heat transfer along an isothermal single vertical plate did not agree with the results for the current measurements; however, the non-similarity model of Chen and Eichhorn [C.C. Chen, R. Eichhorn, Natural convection from a vertical surface to thermally stratified fluid, J. Heat Transfer 98 (1976) 446–451] was in good agreement over most of the wall. There were some discrepancies in the temperature distributions and the heat transfer characteristics, especially at $y/H \geqslant 0.8$ due to the separated flow in this region.

Keywords: Natural convection; Square cavity; Buoyant plume

1. Introduction

The development of plume flows in stratified environments, including free plumes [1] or plumes along a wall [2,3], are of considerable practical interest. In these cases, the buoyancy of the plume is affected by the entrainment of the varying density ambient fluid into the plume. In heated plumes along a heated or cooled vertical wall in a thermally stratified environment, the buoyancy of the plume is also affected by the heat transfer to or from the wall. This type of heated plume commonly occurs in cavities heated on the vertical walls or the vertical and the horizontal walls [4–6], and can be laminar or turbulent depending on a number of factors including the size of the cavity, the temperature of the walls and the Prandtl number of the fluid. Laminar natural convection flow is often observed in smaller cavities [7,8].

The laminar natural convection flow and heat transfer characteristics in cavities heated on the side walls have been studied both experimentally [9–11] and numerically [12,13] for different working fluids and aspect ratio [5,14,15]. The early investigations on this topic have been reviewed [16–18]. Ostrach and Raghavan [19] and Shiralkar and Tien [20] observed that the temperature of the top and bottom walls of the cavity had a significant effect on the stratification inside the cavity that in turn affected the flow pattern and the heat transfer characteristics. Ravi et al. [5] and Wu et al. [6] numerically and experimentally investigated how

* Corresponding author. Tel.: +1 905 525 9140x24998; fax: +1 905 572 7944.
E-mail address: chingcy@mcmaster.ca (C.Y. Ching).

0017-9310/$ - see front matter © 2007 Elsevier Ltd. All rights reserved.
doi:10.1016/j.ijheatmasstransfer.2007.07.022

Nomenclature

A	stratification rate of the ambient air, $a = \mathrm{d}T_\infty/\mathrm{d}y$
$B(y)$	non-dimensional integral of the buoyancy force along the heated vertical wall, $B(y) = \frac{\int_0^\delta \rho_\infty(y) g\beta(y)\cdot[T(x,y)-T_\infty(y)]\cdot \mathrm{d}x}{(T_\mathrm{H}-T_{\infty,0})\rho_\infty(y)\beta(y)g}\left(\frac{g\beta(y)a}{4\nu^2\xi}\right)^{1/4}$
$F_\mathrm{B}(y)$	local buoyancy force along the heated vertical wall, $F_\mathrm{B}(y) = \rho_\infty(y)\cdot g\cdot\beta(y)\cdot[T(x,y) - T_\infty(y)]$
g	gravity constant, m/s^2
$Gr(y)$	local Grashof number, $Gr(y) = \frac{g\beta(T_\mathrm{H}-T_\infty(y))y^3}{\nu^2}$
Gr_L	horizontal Grashof number, $Gr_\mathrm{L} = \frac{g\beta(T_\mathrm{H}-T_\mathrm{C})L^3}{\nu^2}$
$h(y)$	local heat transfer coefficient, W m^{-2} K^{-1}
H	height of the cavity, m
K	thermal conductivity of the air, W m^{-1} K^{-1}
L	width of the cavity, m
$M(y)$	non-dimensional momentum flux of the boundary layer flow along the heated vertical wall, $M(y) = \frac{\int_0^\delta V\rho_\infty(y)V\cdot \mathrm{d}x}{\rho_\infty(y)\cdot 2^{5/2}\cdot\nu^{1/2}\cdot[g\beta(y)]^{3/4}\cdot(T_\mathrm{H}-T_{\infty,0})^{3/4}\cdot y^{5/4}}$
$Nu(y)$	local Nusselt number, $Nu(y) = \frac{h(y)\cdot y}{k}$
T_B	average temperature of the bottom wall in the cavity, °C
T_C	average temperature of the cooled vertical wall in the cavity, °C
T_H	average temperature of the heated vertical wall in the cavity, °C
T_T	average temperature of the top wall in the cavity, °C
$T_\infty(y)$	local ambient temperature in the central or core region of the cavity, °C
$T_{\infty,0}$	temperature of the ambient air at the height of $y = 0$, °C
V	vertical velocity component of the upward flow along the heated vertical wall, m/s
X	distance from the heated vertical wall, m
Y	height above the bottom wall, m
β	volume expansion coefficient at constant pressure, K^{-1}
η_1	a non-dimensional distance from the heated vertical wall in the similarity solution [26], $\eta_1 = (g\beta/4\nu^2)^{1/4}a^{1/4}x$
η_2	a non-dimensional distance from the heated vertical wall in the non-similarity solution [25], $\eta_2 = (g\beta/4\nu^2)^{1/4}(a/\xi)^{1/4}x$
ν	kinematic viscosity, m^2/s
ρ_∞	density of the ambient air, kg/m^3
θ	non-dimensional temperature, $\theta = (T - T_\mathrm{C})/(T_\mathrm{H} - T_\mathrm{C})$
θ_B	non-dimensional temperature of the bottom wall in the cavity, $\theta_\mathrm{B} = (T_\mathrm{B} - T_\mathrm{C})/(T_\mathrm{H} - T_\mathrm{C})$
θ_C	non-dimensional temperature of the cooled vertical wall in the cavity, $\theta_C = (T_\mathrm{C} - T_\mathrm{C})/(T_\mathrm{H} - T_\mathrm{C})$
θ_H	non-dimensional temperature of the heated vertical wall in the cavity, $\theta_\mathrm{H} = (T_\mathrm{H} - T_\mathrm{C})/(T_\mathrm{H} - T_\mathrm{C})$
θ_T	non-dimensional temperature of the top wall temperature in the cavity, $\theta_\mathrm{T} = (T_\mathrm{T} - T_\mathrm{C})/(T_\mathrm{H} - T_\mathrm{C})$
θ_1	a non-dimensional temperature in the similarity solution [26], $\theta_1 = (T - T_\infty)/(T_\mathrm{H} - T_\infty)$
θ_2	a non-dimensional temperature in the non-similarity solution [25], $\theta_2 = (T - T_{\infty,0})/(T_\mathrm{H} - T_{\infty,0})$
ξ	non-dimensional vertical distance, $\xi = ay/(T_\mathrm{H} - T_{\infty,0})$
δ	thickness of the boundary layer, m

Subscripts

B	bottom wall of the cavity
C	cooled vertical wall of the cavity
H	heated vertical wall of the cavity
T	top wall of the cavity

the change in the temperatures of the top and bottom walls affected the natural convection flow in a square cavity with a moderate temperature difference in the vertical direction. They found that an increase in the temperature of the top wall resulted in a significant change in the flow pattern in the cavity. This was true particularly near the upper corner between the heated walls when the temperature of the top wall was close to or larger than that of the heated vertical wall. In this case, the flow separated from the top wall near the corner due to the formation of a negatively buoyant plume. The development of the plume for higher temperatures has not been investigated experimentally for air flows, though the results from the numerical study [20] suggested the vertical plume may separate below the corner when the temperature of the top wall was much larger than the vertical wall. In particular, the flow formed a recirculating region near the corner when the temperature difference in the vertical direction was five times that in the horizontal direction. There was no evidence of significant oscillation in the plume similar to the observations by Ravi et al. [5] and Wu et al. [6] for the cases with more moderate top wall temperatures.

A number of models have also been developed for the natural convection flows on isolated isothermal vertical walls in stratified environments. For example, Cheesewright [21] developed similarity solutions for the flow along an isothermal plate in non-isothermal ambient air. This included solutions for a range of ambient temperature distributions, but not a linear stable ambient temperature distribution like those observed for the natural convection flows in cavities driven by a temperature difference between the vertical walls [6,11]. Sparrow and co-workers [22–24]

proposed a local non-similarity method that included a second term to account for the changes in the streamwise direction. Chen and Eichhorn [25], later, compared the solutions from this non-similarity approach to the experimental measurements of natural convection from a cylinder in a stratified fluid with a Prandtl number of 6.0 and found good agreement between the experiment and the solution. They examined the flow with a Prandtl number of 0.7 but did not compare the results with experiments. Kulkarni et al. [26] later suggested that there were similarity solutions for the natural convection flow along a vertical wall in a stratified environment with a linear temperature distribution, but did not compare their results with experiments, instead comparing with other similarity and non-similarity solutions. Heretofore, there does not appear to have been any attempts to compare these solutions to experimental results for natural convection of air flows in cavities.

Thus, the objectives of this investigation were twofold. The first is to experimentally study the effect that the top wall temperature had on the buoyant air plume on a heated vertical wall in a square cavity, in particular for larger top wall temperatures where the plume seems to separate from the vertical wall. The second is to compare the predictions from previous similarity and non-similarity models for the natural convection flow along an isothermal vertical wall to the results from the experiments in order to examine if these models can accurately predict the development of the wall plume in these cases.

2. Experimental methodology

The experiments in this investigation were performed in an air-filled square cavity shown in Fig. 1 that was also used by Wu et al. [6]. The cavity was set up so its width and height were both 305 mm. The depth of the cavity was 914 mm, which was three times the height and width, so that the flow should be approximately two-dimensional as suggested in a number of previous studies [11,19]. The walls of this square cavity were designed so that one of the vertical walls and the top wall could be heated independently, while the other vertical wall and the bottom wall were cooled. The ends of the square cavity were sealed using walls with large glass windows so the flow in the cavity could be visualized.

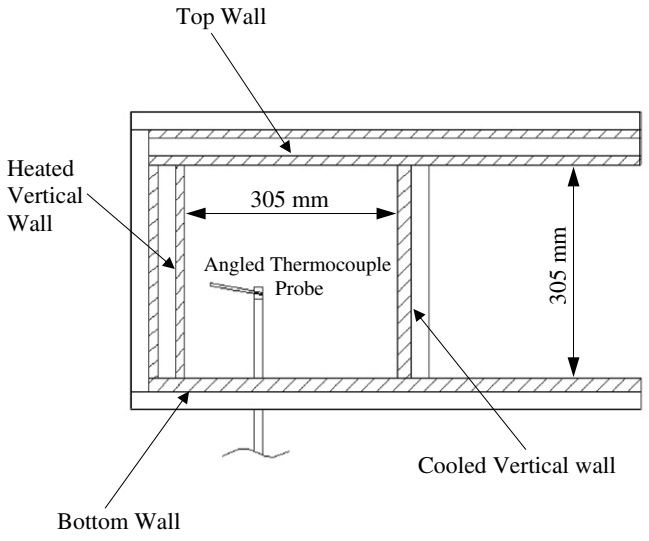

Fig. 1. Schematic of square cavity with heated top and cooled bottom walls.

The top wall and the heated vertical wall were constructed using 12.7 mm thick aluminium plates. The heated vertical wall included three silicone rubber heaters, with a maximum capacity of 180 W, while the top wall included two heaters in the section examined here. Each heater was independently controlled using a multi-channel variable duty controller. Guard walls with seven independent heaters were attached outside these walls to reduce heat loss from the walls. In the current experiments, the heat transfer between the heated vertical wall and its guard wall was less than 15% of the heat transfer into the cavity from the heated vertical wall. The bottom wall and the cooled vertical wall were also constructed from 12.7 mm thick aluminium plates that contained serpentine cooling channels. Municipal water was circulated through the channels to remove the heat from these two plates. The temperature of these walls in this case was kept approximately uniform by maintaining a relatively high cooling water flow rate. This was facilitated by the fact that the heat flux through the walls was relatively low in the current investigation. The heated walls were also maintained at a uniform temperature by independently controlling the power to the individual heaters. In all cases, the maximum discrepancy, which occurred near the corner regions, between the local temperature and the average wall temperature was less than 4%. In order to minimize the heat transfer between the heated vertical wall and the top wall, the junction between the walls was insulated using a thin layer of mineral fibre paper. The heated vertical wall was isolated from the bottom wall by supporting its guard wall on four small Delrin blocks so that an air gap of approximately 1 mm high was present. The temperature on the walls of the square cavity was measured using 0.25 mm (0.010″) T-type thermocouples that were embedded in the plates. There were, respectively, 18, 11, 12 and 11 thermocouples embedded in the heated vertical wall, cooled vertical wall, top wall and bottom wall. Among them, 6, 3, 4 and 3 thermocouples were embedded along the centerlines to continuously monitor the changes in the temperatures so that the average wall temperatures reported here can be calculated.

The temperature distribution of the air in the square cavity was measured using two different T-type thermocouples mounted on a two-dimensional traverse. In the first experiments, the temperature was measured with a 0.25 mm (0.010″) diameter T-type thermocouple probe mounted on a 3.2 mm diameter and 63.5 mm long ceramic tube angled at 10° to the horizontal so measurements could be performed in the upper corner region. It was found that

this angled thermocouple probe could not be used to accurately measure the temperature distributions very close to the heated vertical wall. Thus, in the second set of experiments, the air temperature was measured using a 0.051 mm (0.002″) diameter T-type thermocouple mounted between two 1.5 mm diameter tubes that were 57 mm long and 29 mm apart. These tubes were horizontal similar to Wu et al. [6] and the measurements from this probe were

Table 1
Summary of the wall temperatures and Grashof numbers for the cases studied in this investigation

Case	T_H (°C)	T_C (°C)	T_T (°C)	T_B (°C)	θ_H	θ_C	θ_T	θ_B	Gr_L	Type of thermocouple probe
1-a	52	12	69	12	1	0	1.4	0	1.39×10^8	Angled
1-b	52	13	67	13	1	0	1.4	0	1.34×10^8	Horizontal
2-a	51	14	86	14	1	0	1.9	0	1.32×10^8	Angled
2-b	51	14	83	14	1	0	1.9	0	1.32×10^8	Horizontal
3-a	54	12	109	12	1	0	2.3	0	1.44×10^8	Angled
3-b	54	15	106	15	1	0	2.3	0	1.31×10^8	Horizontal

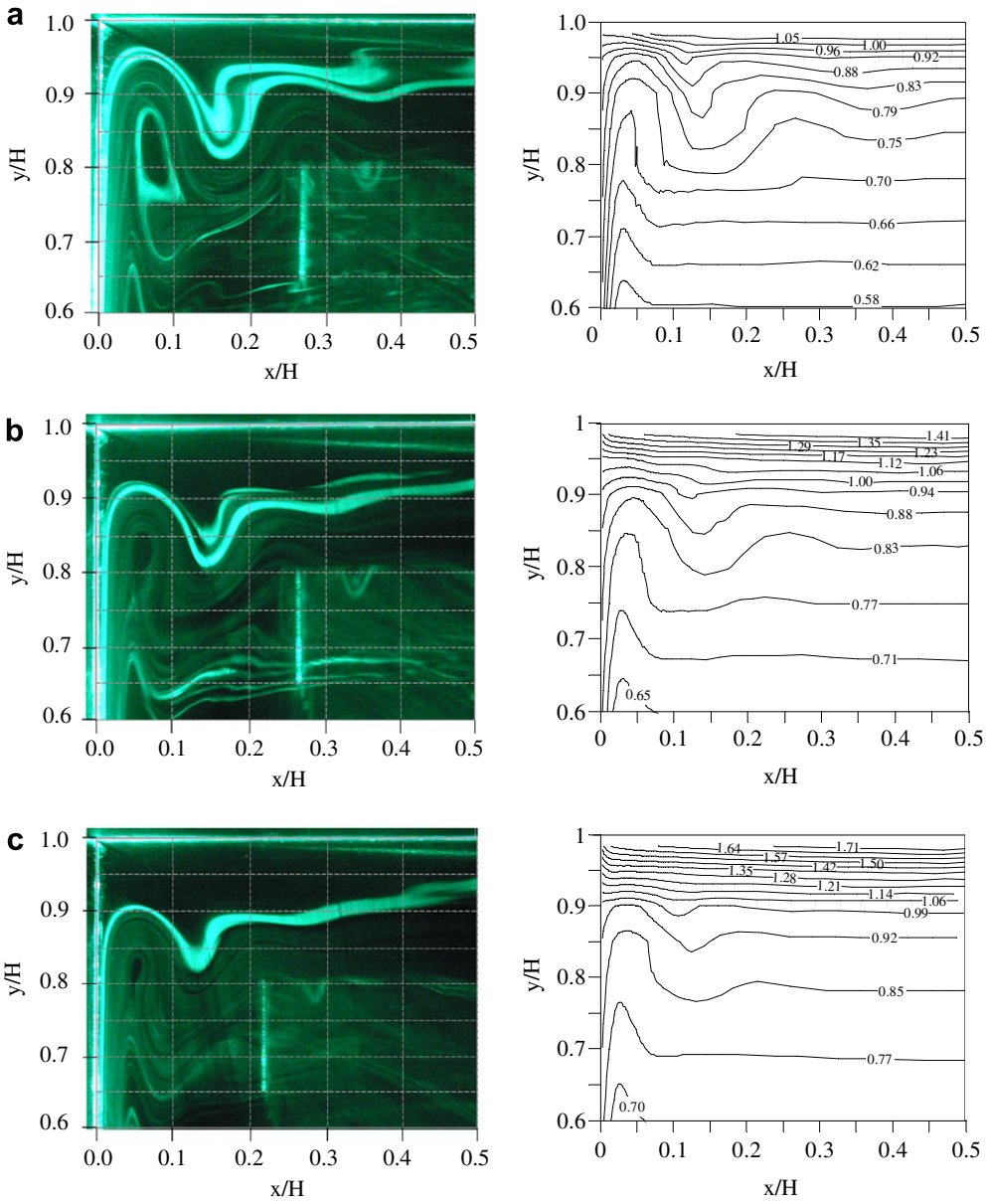

Fig. 2. Flow patterns (left) and temperature contours (right) in the upper left region of the square cavity with non-dimensional top wall temperatures of (a) 1.4, (b) 1.9, and (c) 2.3.

found to be more accurate, especially in the region close to the heated vertical wall. The position of the thermocouple probes relative to the walls for both probes was determined using positioning rods installed in the probe holder that closed an electrical circuit when they touched the wall. Since the temperature changed sharply near the heated vertical wall, the temperature measurements were made at 0.25 mm intervals for the first 6.5 mm from the wall. The distance between consecutive measurement locations was subsequently increased from 0.5 mm to 30 mm as the distance from the wall was increased. For the step size of 0.25 mm, the accuracy of the location of the probe is approximately 0.02–0.03 mm, resulting in an uncertainty in the temperature gradient of about 5%.

In each case, measurements were started after the wall temperatures fluctuated less than ±0.5 °C for over 1 h. The wall temperatures in the two sets of experiments were matched as closely as possible for each case as summarized in Table 1. The instantaneous temperature measurements from the thermocouple probes were averaged for 20 s at each point. The uncertainty in the temperatures measured by the T-type thermocouple probe was ±1 °C, and the uncertainty in the local Nusselt number obtained here was estimated to be 5–8% using the approach outlined by Coleman and Steele [27].

The flow in the square cavity was visualized using incense smoke that was illuminated by a laser light sheet. The smoke was generated by slowly moving air over burning incense. The smoke was cooled to approximately room temperature before it was slowly injected into the cavity through one of the two slots machined in the bottom wall of the cavity for the traverse. A digital camera positioned outside the window of a sidewall of the cavity was used to record the resulting smoke pattern illuminated by a laser light sheet projected into the cavity through the other slot in the bottom wall for the traverse.

3. Results and discussion

The laminar natural convection in an air-filled square cavity was examined for cases where the top wall temperature was significantly larger than the heated vertical wall. The average temperatures of the vertical walls on the two sides of the cavity were maintained at approximately 52 °C and 14 °C, respectively, so the horizontal Grashof number based on the width of the square cavity, Gr_L, was approximately 1.3×10^8. The bottom wall temperature was maintained at approximately 14 °C while the average top wall temperature was varied from 67 °C to 109 °C, corresponding to non-dimensional temperatures of 1.4–2.3.

The flow patterns and the temperature contours in the upper left quarter of the square cavity for three different top wall temperatures are shown in Fig. 2. The temperature contours were generated from the measured temperature profiles using a commercial package. The results show that the natural convection plume travelling along the heated vertical wall separates from the wall before reaching the corner. It is difficult to accurately determine the separation point without quantitative velocity measurements in the near-wall region. However, for this study, it was estimated from the flow visualizations as the point where the upward flow first leaves the vertical wall. The temperature contours provide similar flow field information as the flow visualization, since once the flow separates the convective effects will dominate the diffusive effects. As a result of the flow separation, there is a recirculating flow region between the separated flow and the heated vertical wall similar to the numerical study by Shiralkar and Tien [20]. Here, the plume attaches to the top wall near the opposite corner region as shown in Fig. 3 for a non-dimensional top wall temperature of 2.3. This seems similar to the results in Shiralkar and Tien [20] though they did not state where the plume reattached to the wall. For the smaller non-dimensional top wall temperature, there was some temporal variability in the flow, which reduced as the top wall temperature was increased. The two images shown in Fig. 3, which were taken approximately 15 s apart, show that the flow is steady for the non-dimensional top wall temperature of 2.3. The temperature measurements show that the core region of the cavity is moderately stratified. There is, however, a highly stratified region above the buoyant plume after it separates from the vertical wall. This is different from the results reported by Ravi et al. [5] and Wu et al. [6] for lower non-dimensional top wall temperature where there was evidence of a plume separating from the top wall but not a highly stratified region. The results show that the flow undulates in the vertical direction after turning in the horizontal direction, similar to the results in Wu et al. [6] and Ravi et al. [5]. For the larger top wall temperature examined here, the plume flow passes

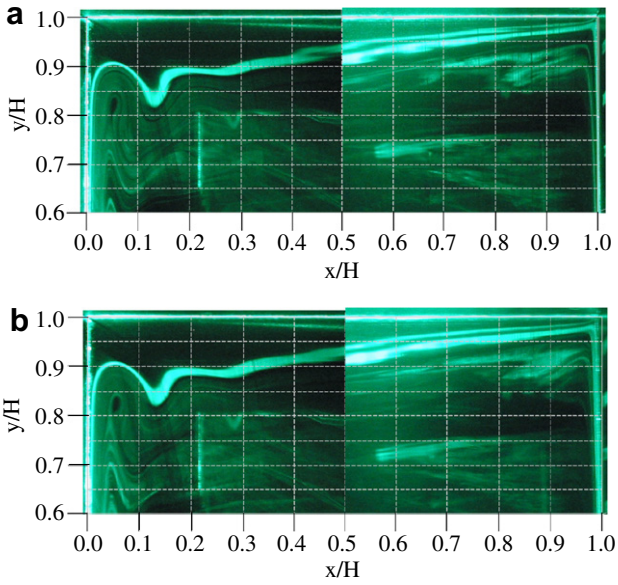

Fig. 3. Typical flow patterns across the entire width of the square cavity with non-dimensional top wall temperature of 2.3. The images (a) and (b) were taken about 15 s apart.

through its neutral buoyancy point and separates from the vertical wall before reaching the top wall so the oscillations occur lower in the cavity. The magnitude of these fluctuations becomes smaller when the top wall temperature increases, indicating the flow becomes more stable with an increase of the top wall temperature. This differed from the numerical results of Shiralkar and Tien [20], where there was no evidence of oscillations in the plume. In that case, the non-dimensional top wall temperature was three times larger than studied here, likely resulting in a larger stratification above the plume which may explain the difference.

The change of the local buoyancy force in the flow along the vertical wall given by

$$F_B(y) = \rho_\infty(y) \cdot g \cdot \beta(y) \cdot [T(x,y) - T_\infty(y)] \quad (1)$$

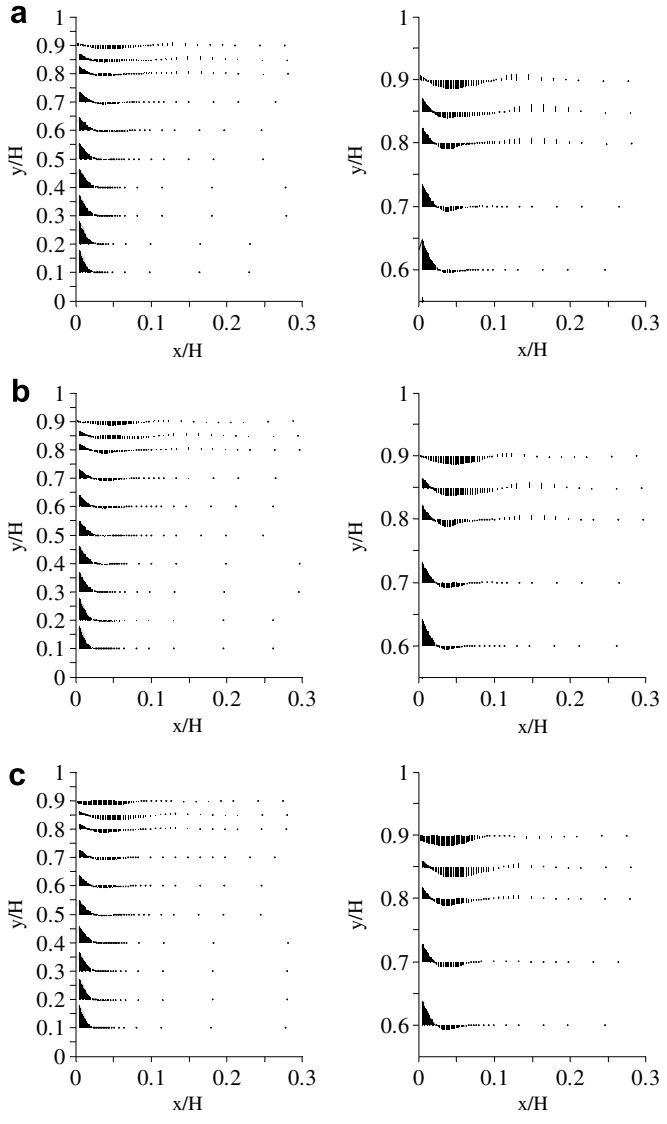

Fig. 4. Changes in the local buoyancy force distributions along the heated vertical wall (left) with an enlarged view in the corner region (right) for non-dimensional top wall temperatures of (a) 1.4, (b) 1.9, and (c) 2.3. The results in the region $y/H \leqslant 0.85$ are from the horizontal thermocouple, while above this region are from the angled thermocouple.

for the different cases are shown in Fig. 4. For clarity, an enlarged view in the region $y/H > 0.6$ is shown on the right in this figure. Here, $\rho_\infty(y)$ and $T_\infty(y)$ are the density and temperature of air in the cavity far from the heated vertical wall, and $\beta(y)$ is determined from $T_\infty(y)$. The profiles in the region below $y/H \leqslant 0.85$ were taken from the measurements with the horizontal thermocouple probe so the results near the vertical wall would be more accurate. The results show that the local buoyancy force decreases with height due to the increase of T_∞ as expected. There are negative local buoyancy forces above $y/H \approx 0.5$ due to the undershoots in the temperature profiles. The negative buoyancy force became larger near the upper corner suggesting that the plume along the vertical wall had passed its neutral buoyancy point. The local buoyancy force at a given height decreases with an increase of the top wall temperature as expected and the region of negative buoyancy near the top wall becomes larger. The plume separates from the wall in this region indicating the negative buoyancy force does play a significant role in affecting the upward motion of the plume.

4. Comparison with models

The measurements of the plume on the heated vertical wall for three different cases were compared to the similarity solution proposed by Kulkarni et al. [26] and the non-similarity solution proposed by Chen and Eichhorn [25]. One limitation of these models is that the stratification rate of the ambient air (in the core region here) must be known *a priori* to solve the equations. In the case of the cavity flow examined here, the stratification rate was determined from the experimental data. The change in temperature at $x/H = 0.5$ with height is shown in Fig. 5. The temperature gradient in the moderately stratified core region is largely

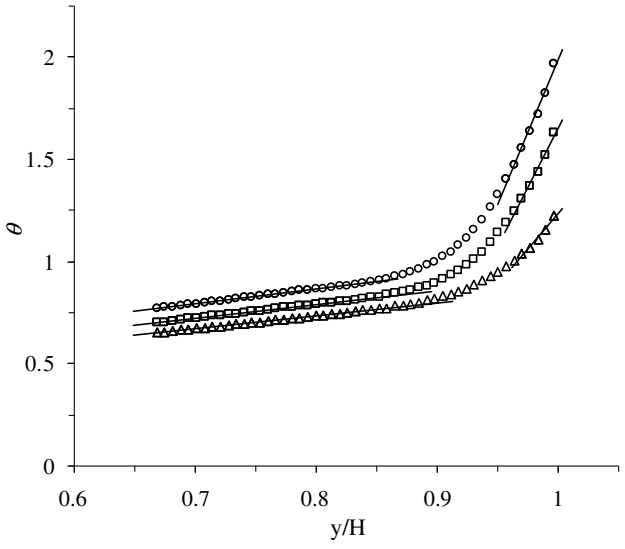

Fig. 5. Comparison of the non-dimensional temperature, θ, at $x/H = 0.5$ for the cases with non-dimensional top wall temperatures of (Δ) 1.4, (□) 1.9, and (○) 2.3.

unaffected by the change in the temperature of the top wall. However, the distance from the top wall to the location where the plume separates from the heated vertical wall increases with the top wall temperature, thereby increasing the size of the highly stratified region near the top of the cavity as noted above.

The non-dimensional temperature profiles in the square cavity determined using the similarity solution of Kulkarni

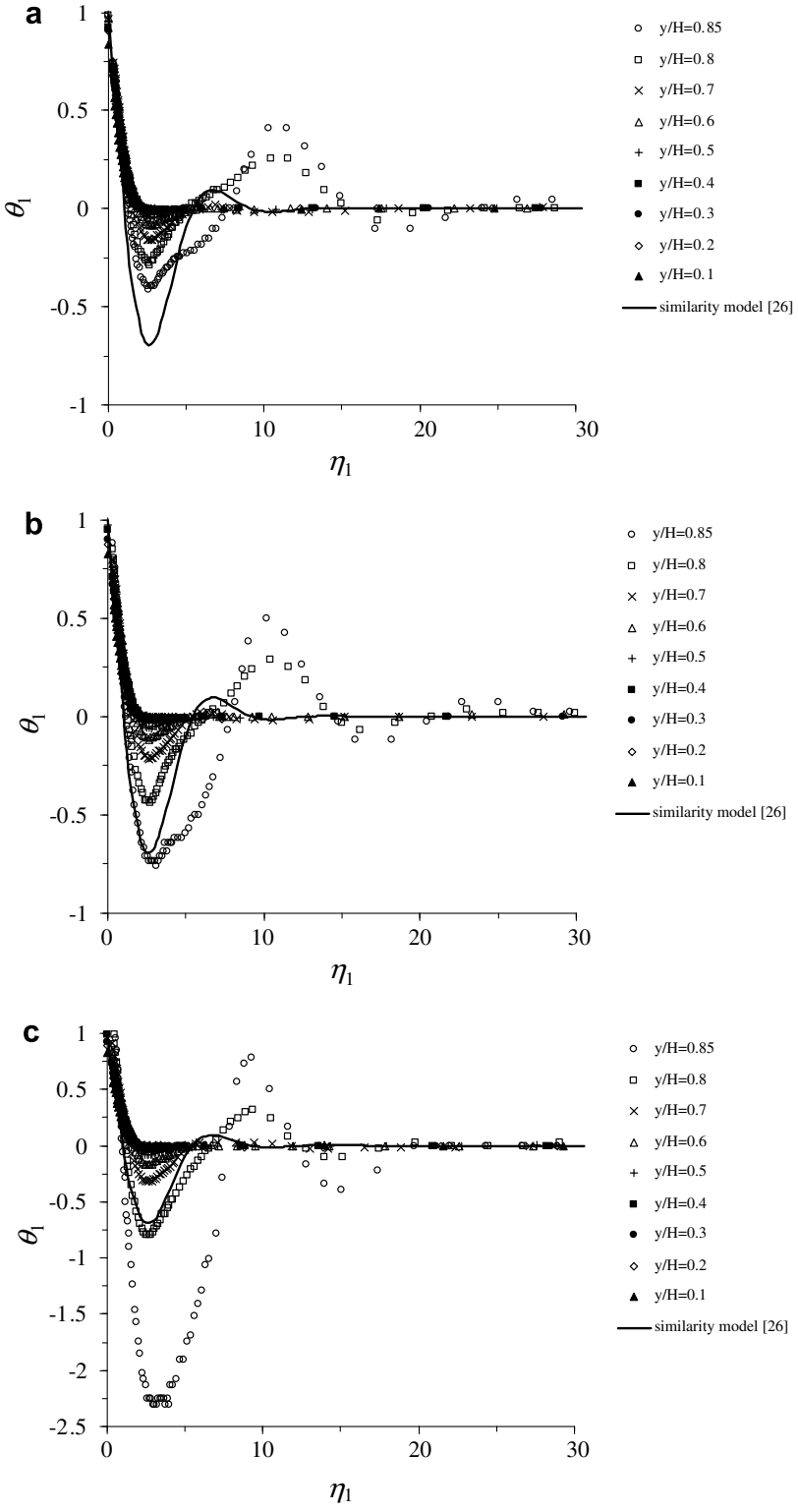

Fig. 6. Comparison of the non-dimensional temperature distributions, θ_1, predicted by the similarity model [26] with the measurements in the square cavity for non-dimensional top wall temperatures of (a) 1.4, (b) 1.9, and (c) 2.3 at the different heights.

et al. [26] for the three different top wall temperatures are shown in Fig. 6 with the corresponding experimental profiles. Here, $\theta_1 = (T - T_\infty)/(T_H - T_\infty)$ is the non-dimensional temperature, and $\eta_1 = (g\beta/4\nu^2)^{1/4} a^{1/4} x$ is the non-dimensional distance from the heated vertical wall, where a is the stratification rate of the ambient temperature. The results show that the similarity solution presented by Kulkarni et al. [26] does not describe the current cases. For the cases where θ_T was 1.4 or 1.9, the experimental temperature distributions approached the profile predicted by the similarity solution but did not reach this profile. When θ_T was 2.3, the temperature profile at $y/H = 0.85$ overshot the profile predicted by the similarity solution indicating that the similarity solution may not represent a stable equilibrium solution for this flow. The integral of the buoyancy for the thermal boundary layer determined from the similarity solution was negative for air flow. Thus, the similarity solution can at most describe a decelerating plume after it has passed through the neutral buoyancy point and this does not seem to be the case. It should be noted this is different from the results for higher Prandtl number fluids where the integral of the buoyancy for the plume determined from the similarity solution [26] is positive. The similarity solution may better describe the flows in those cases.

Comparisons of the profiles predicted by the non-similarity model outlined in Chen and Eichhorn [25] and the non-dimensional temperature profiles along the heated vertical wall obtained from the measurements for the three different top wall temperatures are shown in Fig. 7. Here, $\theta_2 = (T - T_{\infty,0})/(T_H - T_{\infty,0})$ is a non-dimensional temperature where $T_{\infty,0}$ is the temperature of the ambient air at the height of 0 and $\eta_2 = (g\beta/4\nu^2)^{1/4}(a/\xi)^{1/4} x$ is a non-dimensional distance from the heated vertical wall. This model includes a parameter ξ given by $\xi = ay/(T_H - T_{\infty,0})$ that accounts for changes in the streamwise direction. The temperature profiles from the non-similarity model in the region $y/H < 0.5$ are in good agreement with the measurements. In the upper part of the heated vertical wall, there are some discrepancies between the experimental data and the profiles from the model. This is particularly true in the region $y/H \geqslant 0.8$ near the edge of the plume at the large top wall temperatures where the plume separates from the wall. The non-uniformity in the experimental temperature profiles was due in part to the undulation in the plume after it separates from the vertical wall that was not considered in the model.

One question of interest is whether the temperature profiles for the non-similarity model can accurately predict the heat transfer from the heated vertical wall. This was examined by comparing the non-dimensional temperature gradient on the surface of the wall from the non-similarity solution given by

$$-\theta_2'\big|_{\eta_2=0} = Nu(y) \cdot Gr(y)^{-1/4} \cdot \left(\frac{T_H - T_\infty}{T_H - T_{\infty,0}}\right)^{5/4} \cdot \sqrt{2}, \qquad (2)$$

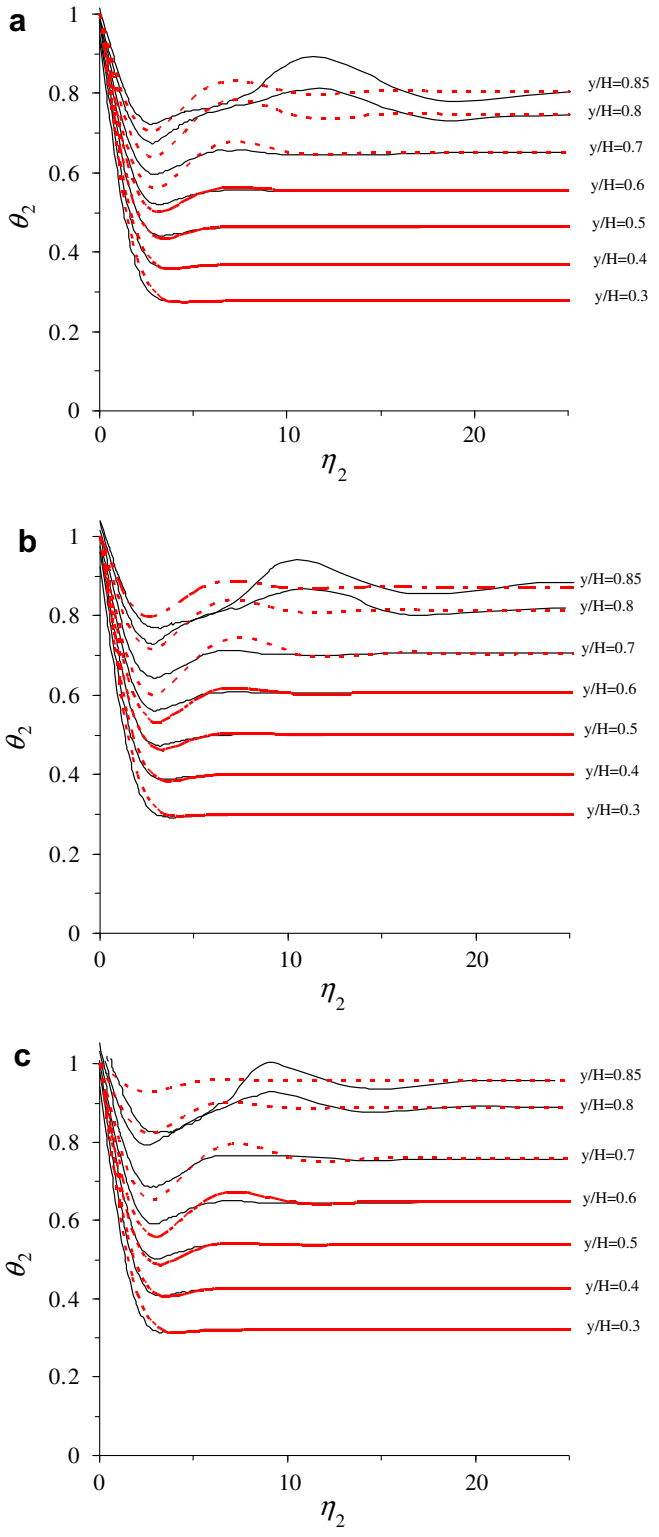

Fig. 7. Comparison of the non-dimensional temperature profiles - - - predicted by the non-similarity model [25] and — from the measurements in the square cavity for non-dimensional top wall temperatures of (a) 1.4, (b) 1.9, and (c) 2.3.

where $Nu(y)$ is the local Nusselt number and $Gr(y)$ is the local Grashof number. The results in Fig. 8 show that the predictions from the non-similarity solution in the region

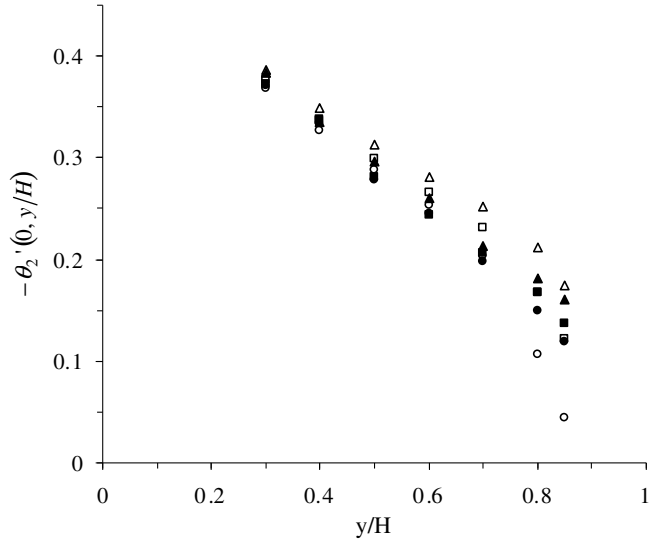

Fig. 8. Comparison of the non-dimensional temperature gradient at the surface of the heated vertical wall, $-\theta_2'(0, y/H)$, from the non-similarity model [25] (open) and the experimental data (solid) with non-dimensional top wall temperatures of (Δ) 1.4, (□) 1.9, and (○) 2.3.

$y/H \geqslant 0.5$ were slightly larger than the measurements. There were also differences in the region $y/H \geqslant 0.8$ for the case where θ_T was 2.3, again likely due to the secondary flow region that could not be predicted in the model. Overall, though, the agreement is quite good.

The accuracy of the model in predicting the upward flow along the heated vertical wall can also be examined by comparing the change in the non-dimensional integral of the buoyancy force along the heated vertical wall given by

$$B(y) = \frac{\int_0^\delta \rho_\infty(y) g\beta(y) \cdot [T(x,y) - T_\infty(y)] \cdot \mathrm{d}x}{(T_H - T_{\infty,0})\rho_\infty(y)\beta(y)g} \left(\frac{g\beta(y)a}{4\nu^2\xi}\right)^{1/4} = \int_0^\delta \theta_2 \cdot \mathrm{d}\eta_2. \tag{3}$$

The results for the three different top wall temperatures are shown in Fig. 9. The non-dimensional integral of the buoyancy force, $B(y)$, decreased along the heated vertical wall due to the increase in T_∞ with height. There were some differences in the buoyancy for $y/H > 0.8$ as expected. The model predictions and measurements were in reasonable agreement and the model seemed to capture some trends in the data. In particular, the model seemed to reasonably predict the change in buoyancy when the temperature of the top wall increased. The buoyancy for the non-similarity model decreased more rapidly with height than the experimental data, suggesting the model does not capture all of the features from the measurements. It is not clear if this was from differences in the initial thermal boundary layer.

The change in the non-dimensional momentum flux of the boundary layer flow along the heated vertical wall from the non-similarity model developed by Chen and Eichhorn [25] given by

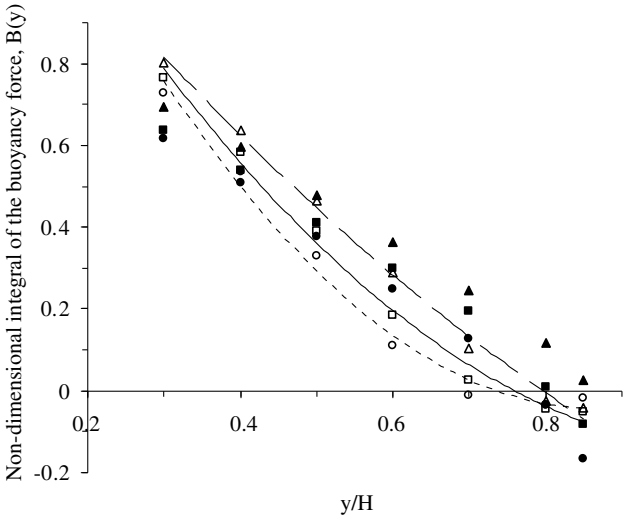

Fig. 9. Comparison of the non-dimensional integral of the buoyancy force across the plume along the heated vertical wall, $B(y)$, from the non-similarity model [25] (open) and the experimental data (solid) with non-dimensional top wall temperatures of (Δ) 1.4, (□) 1.9, and (○) 2.3.

$$M(y) = \frac{\int_0^\delta V\rho_\infty(y)V \cdot \mathrm{d}x}{\rho_\infty(y) \cdot 2^{5/2} \cdot \nu^{1/2} \cdot [g\beta(y)]^{3/4} \cdot (T_H - T_{\infty,0})^{3/4} \cdot y^{5/4}} \tag{4}$$

for the three different cases is shown in Fig. 10. Here, the momentum flux can be expressed in terms of a dimensionless stream function that can be solved to estimate the momentum flux without the velocity distributions [25]. The momentum flux decreased with the height, approaching zero at a location near the top wall. This occurred more rapidly with the larger top wall temperature as expected. The model cannot actually predict the location where the flow separates from the vertical wall but it can be inferred from the location where the momentum approached zero. This location is similar to the maximum height of the

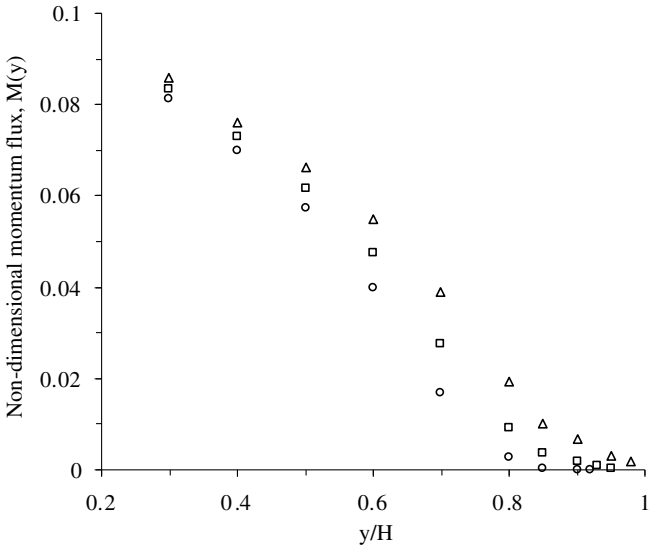

Fig. 10. Comparison of the non-dimensional momentum flux of the plume along the heated vertical wall, $M(y)$, predicted from the non-similarity model [25] for non-dimensional top wall temperatures of (Δ) 1.4, (□) 1.9, and (○) 2.3.

plume in the measurement at least for the largest top wall temperature. For the lower top wall temperatures, the pressure gradient induced by the recirculating flow in the corner region should be affecting the flow in the corner.

5. Conclusions

An experimental investigation was performed to characterize the laminar natural convection in an air-filled square cavity heated and cooled on the vertical walls for cases where the top wall temperature was larger than the heated vertical wall. The experiments were performed for a horizontal Grashof number of approximately 1.3×10^8, and non-dimensional top wall temperatures in the range 1.4–2.3. Flow visualizations and temperature measurements showed that the natural convection plume on the heated vertical wall separated from this wall due to the negative buoyancy imposed by the stratification. As a result, three different regions were formed in the cavity with the top wall temperature significantly larger than the heated vertical wall temperature: a stratified core region, a buoyant plume flow region, and a highly stratified region above the plume after it separated from the vertical wall. The results showed that the highly stratified region became larger and more stable as the top wall temperature increased, so the penetration of the plume into this region became smaller. The temperature distribution in the core region below the location where the plume separated was largely unaffected by the change in the top wall temperature.

The temperature profiles predicted from the similarity solutions for the natural convection along an isothermal vertical wall in a stratified medium proposed by Kulkarni et al. [26] do not agree with the measurements in the current cases. The buoyancy associated with the temperature profiles predicted from similarity solutions were negative so they could, as most, describe a decelerating plume after it has passed through the neutral buoyancy point. The plumes here either did not reach the solutions or overshot them depending on the top wall temperature. The profiles predicted using the non-similarity model outlined in Chen and Eichhorn [25] were in reasonable agreement with the measurements in the region below the point where the plume separated from the vertical wall. The heat transfer from the heated vertical wall was reasonably predicted by the non-similarity model but there were some differences in the non-dimensional integral of the buoyancy force along the heated vertical wall between the experimental data and the non-similarity solutions.

Acknowledgement

The support of the Natural Sciences and Engineering Research Council (NSERC) of Canada is gratefully acknowledged.

References

[1] L.J. Bloomfield, R.C. Kerr, Turbulent fountains in a stratified fluid, J. Fluid Mech. 358 (1998) 335–356.
[2] P.G. Baines, Mixing in flows down gentle slopes into stratified environments, J. Fluid Mech. 443 (2001) 237–270.
[3] P.G. Baines, Two-dimensional plume in stratified environments, J. Fluid Mech. 471 (2002) 315–337.
[4] G.K. Batchelor, Heat transfer by free convection across a closed cavity between vertical boundaries at different temperatures, Quart. Appl. Math. 12 (1954) 209–233.
[5] M.R. Ravi, R.A.W.M. Henkes, C.J. Hoogendoorn, On the high-Rayleigh-number structure of steady laminar natural-convection flow in a square enclosure, J. Fluid Mech. 262 (1994) 325–351.
[6] W. Wu, D. Ewing, C.Y. Ching, The effect of the top and bottom wall temperatures on the laminar natural convection in an air-filled square cavity, Int. J. Heat Mass Transfer 49 (2006) 1999–2008.
[7] J.W. Elder, Laminar free convection in a vertical slot, J. Fluid Mech. 23 (1965) 77–98.
[8] N. Ramesh, S.P. Venkateshan, Experimental study of natural convection in a square enclosure using differential interferometer, Int. J. Heat Mass Transfer 44 (2001) 1107–1117.
[9] E.R.G. Eckert, W.O. Carlson, Natural convection in an air layer enclosed between two vertical plates with different temperatures, Int. J. Heat Mass Transfer 2 (1961) 106–120.
[10] S.H. Yin, T.Y. Wung, K. Chen, Natural convection in an air layer enclosed within rectangular cavities, Int. J. Heat Mass Transfer 21 (1978) 307–315.
[11] Y.S. Tian, T.G. Karayiannis, Low turbulence natural convection in an air filled square cavity. Part I: the thermal and fluid flow fields, Int. J. Heat Mass Transfer 43 (2000) 849–866.
[12] D.E. Cormack, L.G. Leal, J.H. Seinfeld, Natural convection in a shallow cavity with differentially heated end walls. Part 2. Numerical solutions, J. Fluid Mech. 65 (1974) 231–246.
[13] J.E. Drummond, S.A. Korpela, Natural convection in a shallow cavity, J. Fluid Mech. 182 (1987) 543–564.
[14] R.K. Macgregor, A.F. Emery, Free convection through vertical plate layers – moderate and high Prandtl number fluids, J. Heat Transfer 91 (1969) 391–403.
[15] N. Seki, S. Fukusako, H. Inaba, Visual observation of natural convection flow in a narrow vertical cavity, J. Fluid Mech. 84 (1978) 695–704.

[16] C.J. Hoogendoorn, Natural convection in enclosures, in: Proceedings of the Eighth International Heat Transfer Conference, vol. 1, San Francisco, USA, 1986, pp. 111–120.
[17] S. Ostrach, Natural convection in enclosures, J. Heat Transfer 110 (1988) 1175–1190.
[18] J.M. Hyun, Unsteady buoyant convection in an enclosure, Adv. Heat Transfer 24 (1994) 277–320.
[19] S. Ostrach, C. Raghavan, Effect of stabilizing thermal gradients on natural convection in rectangular enclosures, J. Heat Transfer 101 (1979) 238–243.
[20] G.S. Shiralkar, C.L. Tien, A numerical study of the effect of a vertical temperature difference imposed on a horizontal enclosure, Numer. Heat Transfer 5 (1982) 185–197.
[21] R. Cheesewright, Natural convection from a plane, vertical surface in non-isothermal surroundings, Int. J. Heat Mass Transfer 10 (1967) 1847–1859.
[22] E.M. Sparrow, H. Quack, C.J. Boerner, Local nonsimilarity boundary-layer solutions, AIAA J. 8 (1970) 1936–1942.
[23] E.M. Sparrow, H.S. Yu, Local non-similarity thermal boundary-layer solutions, J. Heat Transfer 93 (1971) 328–334.
[24] W.J. Minkowycz, E.M. Sparrow, Local nonsimilar solutions for natural convection on a vertical cylinder, J. Heat Transfer 96 (1974) 178–183.
[25] C.C. Chen, R. Eichhorn, Natural convection from a vertical surface to thermally stratified fluid, J. Heat Transfer 98 (1976) 446–451.
[26] A.K. Kulkarni, H.R. Jacobs, J.J. Hwang, Similarity solution for natural convection flow over an isothermal vertical wall immersed in thermally stratified medium, Int. J. Heat Mass Transfer 30 (1987) 691–698.
[27] H.W. Coleman, W.G. Steele, Experimentation and Uncertainty Analysis for Engineers, second ed., Wiley, New York, 1999, pp. 48–50.